Vol. 14 No. 1
1 9 9 8 Chemical Research in Chinese Universities 70~75

Novel Highly Branched Polyester Nanoparticles(I)*
——Light-Scattering Characterization

MA Rong-Jiu**
(*Polymer Institute, Jilin University, Changchun*, 130023)
WU Qi(Chi)
(*Department of Chemistry, the Chinese University of Hong Kong, Shatin, N.T., Hong Kong*)

(Received Nov. 11, 1996)

Highly branched polyester nanoparticles (HBPN) with a weight-averaged molecular weight of 1.2×10^4 g/mol and a hydrodynamic radius of 4.3 nm were prepared by the polycondensation of phthalic anhydride and pentaerythritol at 142 ℃ under vacuum. The laser light-scattering (LLS) characterization of HBPN in both *N*,*N*-dimethylformamide (DMF) and the buffer (pH =12) was accomplished. DMF is a good solvent for HBPN and there is no aggregation or association between individual particles of HBPN in DMF at room temperature. In the buffer, there exists a very small amount of HBPN aggregates whose size is about 10 times larger than that of individual HBPN particles. There is a balance between individual HBPN particles and the HBPN aggregates, so that HBPN is stable in the buffer and most of HBPN remain as individual particles. The particle size of HBPN can be controlled by the copolymerization time. A combination of static and dynamic LLS results, *i.e.*, M_w and R_h, enables us to estimate that on average each HBPN particle (dentritic-like cluster) contains 4 layers or generation.

Keywords Branched polymer, Nanoparticles, Laser light scattering, Characterization

Introduction

A great number of aqueous-based systems in nature and commodity production contain one type or many types of polymer(s) and surfactant(s) in the same solution, such as a multitude of biological systems, *e.g.*, membranes (structure and functioning) and carriers (lipid transport), and other commerce systems including foods, pharmaceuticals, cosmetics and detergents. Owing to their many important properties, such as rheology control, viscosity enhancement, gels, solubilization, enhanced water solubility, separation and purification of soluble polymers, control of drug delivery, surface activity, adsorption and surface conditioning, the polymer and surfactant systems have found important application, such as clay flocculation[1], mineral floatation including coal floatation[2], polymer solubilization[3], biopolymer conformational changes[4] and enhanced oil recovery[5]. Most of these properties can be attributed to different interactions between the polyelectrolytes chain and surfactant. Therefore, a better understanding of these polymer/surfactant interactions is essential to control and apply these properties. A number of theoretical and experimental studies have been conducted on the interactions between linear polyelectrolyte chains and surfactants[6]. A systemic study of the interactions between highly branched polyelectrolytes and surfactants

* Supported by the National Natural Science Foundation of China and Doctoral Research Foundation of National Education Commission.

** To whom correspondence should be addressed.

is comparatively lack. In this work, highly branched polyester nanoparticles were prepared and characterized by both static and dynamic laser light scattering (LLS). Their stability in the buffer (pH=12) was studied. The correlation between the particle size and reaction time was established. This study has laid a reliable foundation for further studying the interactions between the spherical polyelectrolytes and surfactants.

Experimental

1 Sample Preparations

A type of pseudo-dendritic polymer cluster, highly branched polyester nanoparticles (HBPN), were prepared by a condensation of pentaerythritol and phthalic anhydride molten in a glycerine bath at 142 ℃ under vacuum. The reaction mixture was stirred with a speed adjusted stirrer according to the viscosity of the reaction mixture. The molar ratio of the pentaerythritol to phthalic anhydride was 1 : 2.5. Thus, some of the carboxylic groups in phthalic anhydride still remained when the reaction was completed. The typical reaction time was about 130 minutes. Before reaching its gelation threshold, the reaction vessel was immersed into ice water to stop the reaction. The product was very quickly removed and then dried out under vaccum.

The analytical grade *N*,*N*-dimethylformamide (DMF) from Riedel deHaen was purified and then dried with carbon sieve before use. The diluted solution of HBPN in DMF was prepared by dissolving a proper amount of HBPN in DMF at room temperature for at least one day. After complete dissolution, the solution was clarified by a Whatman filter (Anotop 25, average pore size 0.1 μm) in order to remove dust. The final solution was split into two parts, one was for laser light scattering measurements; the other for the specific refractive index increment(dn/dc) measurement.

The buffer (pH = 12) was prepared by a standard procedure (FIXAMAL Riedel-deHaën). The HBPN alkaline solution was prepared through the following procedure. First, a proper amount of HBPN was dissolved in the buffer; and then the solution was filtered into a dust free scattering cell. The time between the addition of HBPN and the first LLS measurement was half an hour. All the aqueous solutions used in this study were clarified by a millipore 0.2 μm PTFE filter which was treated with methanol before use.

2 Laser Light Scattering (LLS)

A slightly modified commercial spectrometer (ALV/SP-150 equipped with ALV-5000 multitau digital correlator) was used with a solid-state laser (ADLAS DPY425II, output power≈400 MW at λ=532 nm) as the light source. The incident beam was vertically polarized with respect to the scattering plane. A compensated beam attenuator (Newport M-925B) was used to regulate the incident laser light intensity so that a possible localized heating in the light scattering cuvette can be avoided. In static LLS, the precise dn/dc value at 25 ℃ and λ=532 nm was determined by using a recently developed high precision differential refractometer[7]. In dynamic LLS, the intensity-intensity time correlation functions were measured. The correlation functions were accumulated until photon counts in the baseline exceeded 10^6 per channel. The difference between measured and the calculated baselines was kept below 0.1%. All the LS experiments were carried out at 25 ℃. The details of LS experiments and instrumentation can be found elsewhere[8].

Results and Discussion

1 Static LLS

For a diluted macromolecule solution or colloidal suspension at concentration $c/(g \cdot mL^{-1})$, the angular dependence of the excess absolute average scattered intensity, known as the excess Rayleigh ratio $[R_{vv}(q)]$, can be approximately expressed as[9]

$$\frac{Kc}{R_{vv}(q)} \approx \frac{1}{M_w}\left(1 + \frac{1}{3}\langle R_g^2\rangle q^2\right) + 2A_2c \tag{1}$$

where $K = 4\pi^2n^2(dn/dc)^2/(N_A\lambda_0^4)$ with N_A, n and λ_0 are Avogadro's number, the solvent refractive index and the wavelength of light in vacuo, respectively, and $q = (4\pi n/\lambda_0)\sin(\theta/2)$. Eq. (1) shows that in order to get a correct weight-averaged molecular weight (M_w), the precise value of (dn/dc) is very important.

Fig. 1 shows a typical plot of the refractive index increment(dn) *versus* concentration c for HBPN in DMF, where the error associated with dn has been proved to be less than $\pm 1\%$[7]. dn/dc obtained from the slop of the least-square fitting line in Fig. 1 is 1.27 L/g. After measuring $R_{vv}(q)$ at a set of c and θ, we were able to determine M_w, the Z-averaged radius of gyration ($\langle R_g^2\rangle_z^{1/2}$ or written as R_g) and the second virial coefficient (A_2) from the Zimm plot θ and c extrapolations on a single grid (not shown since it is typical). The size of HBPN is so small that $R_{vv}(q)$ is nearly independent on the scattering angle. Therefore, R_g can not be accurately determined in static LLS. The values of A_2 and M_w are 4.5×10^{-5} mol $\cdot$ mL/q^2 and 1.2×10^4 g/mol, respectively. The positive A_2 shows that DMF is a good solvent of HBPN at room temperature. The value of M_w was confirmed by that from GPC.

2 Dynamic LLS

The intensity-intensity time correlation function $G^{(2)}(q,t)$ in the homodyne mode is related to the normalized electric field time correlation function $g^{(1)}(q, t)$[10], which can be expressed as

$$G^{(2)}(q,t) = A[1 + \beta|g^{(1)}(q,t)|^2] \tag{2}$$

where A is a measured baseline; β a spatial coherence constant depending only on the detection optics and its value ($0 \leqslant \beta \leqslant 1$) reflects the signal-to-noise ratio. It can be shown that $g^{(1)}(q, t)$ is related to the line-width distribution $G(\Gamma)$, which can be expressed as

$$g^{(1)}(q,t) = \int_0^\infty G(\Gamma)e^{-\Gamma t}d\Gamma \tag{3}$$

The Laplace inversion of eq. (3) gives $G(\Gamma)$. In the study, the inversion was done by a Contin program equipped with a ALV-5000 digital time correlator. Γ is normally a function of both c and θ, which can be expressed as

$$\frac{\Gamma}{q^2} = D(1 + K_dc)(1 + f\langle R_g^2\rangle_z q^2) \tag{4}$$

where K_d is the second virial coefficient of diffusion; which provides some information for chain-chain interaction and helps one to identify if the theoretical model is applicable to the type of the system studied, and f a dimensionless number at $c \to 0$ and $\theta \to 0$, $\Gamma/q^2 \to D$. Therefore, with a pair of known K_d and f, we can transfer $G(\Gamma)$ obtained in a finite concentration and at a certain scattering angle into a translational diffusion coefficient distribution $G(D)$.

Fig. 2 shows a typical translational diffusion coefficient distribution $G(D)$ (represented

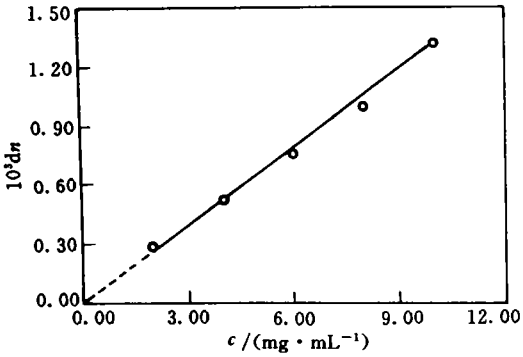

Fig. 1 Plot of the refractive index increment dn *vs.* c_{HBPN}.
t=25 ℃ and λ=532 nm.

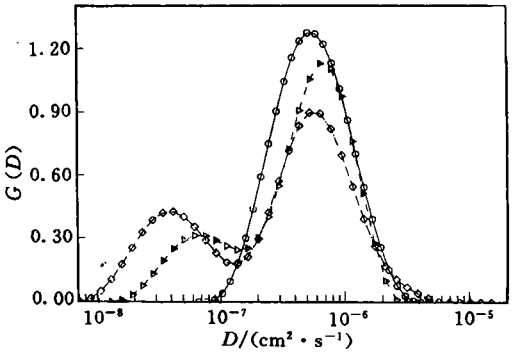

Fig. 2 Translational diffusion coefficient distribution $G(D)$ of HBPN.
t=25 ℃; θ=30℃; (○) c_{HBPN}=2 mg/mL; (△) c_{HBPN}=2 mg/mL; (◇) c_{HBPN}=5 mg/mL.

by "○") of HBPN in DMF at room temperature. In DMF, $G(D)$ has only one peak, indicating that there is no HBPN association or aggregation. The distribution width $\mu\langle D\rangle^2$ is *ca.* 0.36, where $\mu_2=\int_0^\infty G(D)(D-\langle D\rangle)^2 dD$. The polydispersity index M_Z/M_w estimated from $(1+4\mu_2/\langle D\rangle^2)$ is about 2.4, which agrees well with the theoretical prediction ($M_Z/M_w \geqslant 2$ for a polycondensation reaction). This distribution will be very helpful for the further studies of the interactions between HBPN and surfactants.

Fig. 3 shows the HBPN concentration dependence of the averaged translational diffusion coefficient $\langle D\rangle$ for HBPN in DMF at room temperature, where $\langle D\rangle=\int_0^\infty G(D)D dD$, and according to eq. (4), since $qR_g \ll 1$ (as mentioned for R_g above) eq. (4) can be reduced to Yamakawa eqation in diluted solutions

$$\langle D\rangle = D_0(1 + K_d c) \tag{5}$$

From the intercept D_0 we have the translational diffusion coefficient $\langle D\rangle_{c\to 0}=6.4\times10^{-7}$cm^2/s

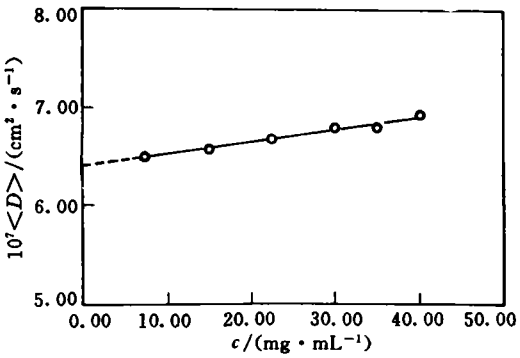

Fig. 3 Concentration dependence of $\langle D\rangle$ of HBPN.
t=25 ℃; θ=90°; $\langle D\rangle=6.40\times10^{-7}[1+2.1c]$.

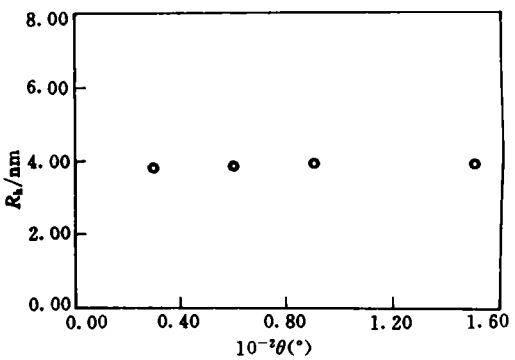

Fig. 4 Angular dependence of the average hydrodynamic radius R_h of HBPN.
t=25 ℃ and c_{HBPN}=6 mg/mL.

and from the slope we have $K_d \approx 2.1$ mL/g on the basis of eq. (5). $\langle D \rangle$ can be further converted into a hydrodynamic radius R_h by using the Stokes-Einsten equation,

$$R_h = \left(\frac{k_B T}{6\pi\eta}\right) D^{-1} \tag{6}$$

where k_B, T and η are the Boltzmann constant, the absolute temperature and the solvent viscosity, respectively. Fig. 4 shows that the angular dependence of the hydrodynamic radius R_h of HBPN in DMF. R_h is independent of the scattering angle in the range of 30°—150°, which is expected on the basis of eq. (4) since the particle size is only *ca.* 4 nm. After knowing K_d and no angular dependence of R_h, we can determine the particle size of HBPN at only one diluted concentration and one scattering angle hereafter.

Since the polycondensation of pentaerythritol and phthalic anhydride is known to be alternatively performed between the hydroxyl group in pentaerythritol and the anhydride group in phthalic anhydride, a combination of the results of static and dynamic LLS as well as acid-base titrimetry showed that the averaged layers or generations in HBPN are about 4 and there are *ca.* 38 unreacted carboxyl groups on its surface, which is in agreement with the theoretical estimation of HBPN structure by means of the known monomer molecular mass and the bond lengths as well as bond angles of both monomers.

Fig. 2 also shows the translational diffusion coefficient distributions $G(D)$ of HBPN in the buffer (pH=12) at 30°, where the triangles and diamonds represent $c_{HBPN}=2$ mg/mL, and $c_{HBPN}=5$ mg/mL, respectively. In the buffer the translational diffusion coefficient distribution of HBPN showed two peaks. The larger peak corresponds to individual HBPN particles, while the smaller peak is related to the HBPN aggregates. The position of the larger peak is nearly independent of c and close to that in DMF. For the smaller peak, as c_{HBPN} increased, not only the area under the peak increased, but also the peak position shifted to the lower D(large size) direction, which further shows that this small peak is related to some kind of larger HBPN aggregates in the buffer. It should be noted that $G(D)$ is an intensity distribution, *i.e.*, the peak area is proportional to the scattered light intensity from the related scatterers, or in other words, the peak area is proportional to $M_w(\propto f_n(M)M^2)$ on the basis of eq. (1), where $f_n(M)$ is the differential number distribution. Fig. 2 shows that the

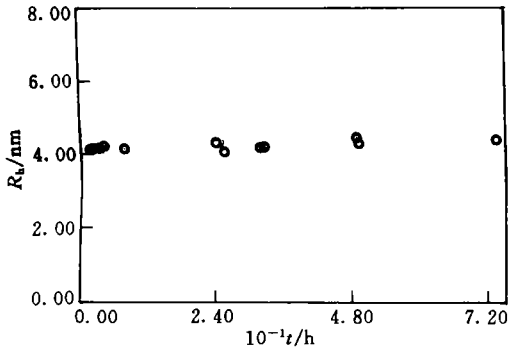

Fig. 5 Stability of HBPN in the buffer (pH=12) in terms of R_h *versus* the standing time t.

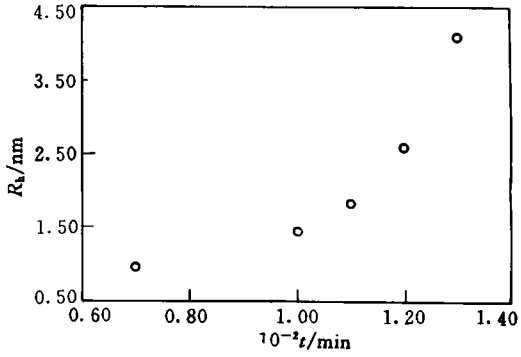

Fig. 6 Particle size of HBPN as a function of the copolymerization time t.
t = 142 ℃, under vacuum; the molar ratio of Pentaerythritol/phthalic anhydride is 1 : 2.5.

size of the HBPN aggregates is *ca.* 10 times larger than that of individual HBPN clusters. This means that the intensity of the scattering of each aggregate is 10^4—10^6 times higher than that of each HBPN cluster if we assume that $M \propto R_h^2$(coil) or R_h^3(uniform sphere). Therefore, the small peak in Fig. 2 actually represents a very small amount of the HBPN aggregates in terms of number.

At molecule level, the carboxylic groups on the HBPN surface are hydrophilic in the buffer. It is this hydrophilic nature that enables HBPN to dissolve in water. However, the rest of HBPN surface is hydrophobic which leads to the observed aggregation. There is a delicate hydrophilic and hydrophobic balance in the HBPN buffer solution. Fig. 5 shows the stability of HBPN in the buffer (pH=12). It clearly demonstrates that HBPN in the buffer is quite stable and the hydrodynamic radius is nearly a constant for several days, which shows that the balance between individual HBPN clusters and aggregates is well kept. This stability is crucial for further studies of the interactions between HBPN and surfactants.

Fig. 6 shows the particle size of HBPN as a function of the copolymerization time at t=142 ℃ under vacuum, where the molar ratio of pentaerythritol/phthalic anhydride is 1 : 2.5. As expected, the size of HBPN increases with the reaction time, especially, near the gelation threshold (about 140 min), which shows that the size of HBPN can be controlled by the reaction time. It should be noted that the polycondensation reaction has to be stopped before reaching its gelation threshold. Otherwise, the crosslinked polyester particles will not be able to dissolve in either DMF or the buffer.

References

[1] Hanna, H. S., Somasundaran, P. J., J. Colloid Interface Sci. **70**, 181(1979)
[2] Przhegorlinskaja, R. W., Zubkava, Yu. N., Khim. Tuer. Topl. (Moskow) **12**, 125(1978)
[3] Jones, M. N. J., Colloid Interface Sci., **23**, 36(1967)
[4] Satake, I., Yang, J. T., Biochem. Biophys. Res. Commun. **54**, 930 (1973)
[5] Taber, J. J., Pure Appl. Chem., **52**, 1 323(1980)
[6] Fundin, J., Brown, W., Macromolecules, **27**, 5 024(1994)
[7] Wu, C., Xia, K. Q., Rev. of Sci. Instruments, **65**, 587(1993)
[8] Wu, C., Woo, K. F., Luo, X. L., Ma, D. Z., Macromolecules, **27**, 6 055(1994)
[9] Zimm, B. H., J. Chem. Phys., **16**, 1 099(1948)
[10] Chu, B., Laser Light Scattering(2nd Ed.), New York: Academic Press, 1991